



RESEARCH ARTICLE

10.1002/2014WR016534

Global sensitivity analysis of the radiative transfer model

Maheshwari Neelam¹ and Binayak P. Mohanty¹

¹Department of Biological and Agricultural Engineering, Texas A&M University, College Station, Texas, USA

Key Points:

- Energy rich environments are more prone to parameter interactions
- Fixed look-up table for parameters will undermine the soil moisture accuracy
- Brightness temperature is more sensitivity to roughness parameters in wet soils

Correspondence to:

B. P. Mohanty,
bmohanty@tamu.edu

Citation:

Neelam, M., and B. P. Mohanty (2015), Global sensitivity analysis of the radiative transfer model, *Water Resour. Res.*, 51, doi:10.1002/2014WR016534.

Received 9 OCT 2014

Accepted 2 MAR 2015

Accepted article online 10 MAR 2015

Abstract With the recently launched Soil Moisture Active Passive (SMAP) mission, it is very important to have a complete understanding of the radiative transfer model for better soil moisture retrievals and to direct future research and field campaigns in areas of necessity. Because natural systems show great variability and complexity with respect to soil, land cover, topography, precipitation, there exist large uncertainties and heterogeneities in model input factors. In this paper, we explore the possibility of using global sensitivity analysis (GSA) technique to study the influence of heterogeneity and uncertainties in model inputs on zero order radiative transfer (ZRT) model and to quantify interactions between parameters. GSA technique is based on decomposition of variance and can handle nonlinear and nonmonotonic functions. We direct our analyses toward growing agricultural fields of corn and soybean in two different regions, Iowa, USA (SMEX02) and Winnipeg, Canada (SMAPVEX12). We noticed that, there exists a spatio-temporal variation in parameter interactions under different soil moisture and vegetation conditions. Radiative Transfer Model (RTM) behaves more non-linearly in SMEX02 and linearly in SMAPVEX12, with average parameter interactions of 14% in SMEX02 and 5% in SMAPVEX12. Also, parameter interactions increased with vegetation water content (VWC) and roughness conditions. Interestingly, soil moisture shows an exponentially decreasing sensitivity function whereas parameters such as root mean square height (RMS height) and vegetation water content show increasing sensitivity with 0.05 v/v increase in soil moisture range. Overall, considering the SMAPVEX12 fields to be water rich environment (due to higher observed SM) and SMEX02 fields to be energy rich environment (due to lower SM and wide ranges of TSURF), our results indicate that first order as well as interactions between the parameters change with water and energy rich environments.

1. Introduction

Soil moisture (SM) plays a fundamental role in governing the hydrological and the terrestrial carbon cycle, and demands a global and consistent monitoring for the future food and water security. Several missions in the past (SSM/I, AMSR-E, and SMOS) have made available satellite-derived soil moisture using both the active and the passive remote sensing. The most commonly used system for modeling the complex soil-vegetation-atmosphere interactions for soil moisture retrieval is described by "Radiative Transfer Equation" (RTE) [Ulaby *et al.*, 1986; Kerr and Njoku, 1990]. Modeling of RTE however requires characterizing the complex land-atmosphere interactions in geophysical parameters which is a difficult task, since land surface parameters show a large heterogeneity, and not all of them are significant in describing the system at all scales. Thus, considering all parameters as significant and incorporating them into the model will result in either an over or an underdetermined system. Therefore, implementing RTE theory into practical soil moisture retrieval algorithm requires reducing the dimensionality by simplifying assumptions without compromising on the system information. This requires us to understand the model behavior and also the parameters which efficiently encapsulate all the processes. A sensitivity analysis (SA) is an effective methodology to attain this objective. SA can result in achieving factor fixing (FF) for noninfluential parameters, or factor prioritization (FP) for important parameters, thereby reducing the output uncertainty. This also reduces number of parameters required for optimization, hereby increasing computational efficiency without undermining the results [Saltelli *et al.*, 2004]. Past studies [Davenport *et al.*, 2005; Crosson *et al.*, 2005; Calvet *et al.*, 2011] have performed sensitivity analysis on brightness temperature to determine the influential parameters using the One-Factor-at-a-Time (OAT) algorithm. This algorithm also called as the Local Sensitivity Analysis (LSA), computes local response of the model by varying a parameter locally while the other input parameters are fixed at their nominal values. LSA only provides a rough estimation of parameter ranking using limited number of model evaluations. These results are, however, qualitative and not quantitative,

and understanding about the underlying model assumptions and processes are restricted in the LSA methods. Also, OAT method is suitable for factor fixing but not for factor prioritization [Saltelli *et al.*, 2008]. In contrast, global sensitivity analysis (GSA) method, comprehensively evaluates model response to variations in inputs in the entire allowable parameter ranges.

In this paper, for the first time we explore the GSA technique in remote sensing arena to evaluate the Zero Order Radiative Transfer (ZRT) model behavior and along with the parameter interactions. We use a variance-based Sobol method which is a widely used GSA technique [Saltelli *et al.*, 2004]. This method quantifies the amount of variance each parameter contributes to the total unconditional variance. Despite its computational demand, it provides a comprehensive sensitivity analysis, and a nonlinear relationship between the parameters. It is important to realize the individual and interaction effects of soil moisture (*SM*), soil texture (Clay fraction (*CF*)), surface roughness (RMS height '*S*' and correlation length '*L*'), vegetation parameters (vegetation water content '*VWC*', vegetation structure '*B*' and scattering albedo '*ω*') on brightness temperature (T_B) to improve model and process understanding. For example, consider the similar scattering and screening effects of surface roughness and vegetation (increase T_B and reduce soil moisture sensitivity) [Njoku and Chan, 2006] which makes it difficult to separate their individual impacts.

We hypothesize that, there exists nonlinear interactions between these parameters which need to be accounted for in modeling. We also hypothesize that, these interactions change with the local climate/climate zones since different parameters come into play under different conditions [Gaur and Mohanty, 2013; Joshi and Mohanty, 2010; Jana and Mohanty, 2012]. An understanding of these spatio-temporal interactions between parameters will result in improved modeling of radiative transfer processes. The objective of this paper is to examine the first order, the second order, and the total sensitivity measures of the ZRT model parameters. We explore this objective under spatio-temporally varying conditions with different wetness conditions and vegetation types. Our study focused on using two field campaigns, Soil Moisture Experiment 2002 (SMEX02) in Iowa and Soil Moisture Active Passive Validation Experiment 2012 (SMAPVEX12) in Winnipeg. Corn and soybean crops are selected for our analysis, since they are the major agricultural crops of the study regions in particular and North America in general. This analysis is carried out in climatologically similar (but locally different) regions such as Iowa, USA, and Winnipeg, Canada. We believe quantification of these interactions of geophysical parameters will help us direct our future soil moisture cal/val campaigns in areas which need more expertise to make accurate retrieval or predictions.

2. Materials and Methods

2.1. Climatology of Iowa and Winnipeg

According to the Koppen climate classification, Iowa and Winnipeg fall under humid continental climate zone [Peel *et al.*, 2007]. Such a climatic region is classified with large seasonal temperature differences, with hot and humid summers and cold severe winters with significant precipitation in all the seasons. Iowa and Winnipeg are categorized as Dfa (high 30s and low 40s latitudes) and Dfb (high 40s and low 50s in latitude) climate zones, respectively. Iowa is mainly characterized by hot summers with an average temperature greater than 22°C in the warmest months and an average temperature above 10°C over a span of 4 months. Winnipeg is characterized by warm summers with warmest month temperature below 22°C and with at least 4 months average temperature above 10°C.

2.2. Soil Moisture Experiment 2002 (SMEX02)

SMEX02 was conducted in central Iowa from 24 June to 12 July, 2002 to validate soil moisture retrieval algorithms for a range of soil and vegetation conditions from aircraft and satellite microwave instruments [Jacobs *et al.*, 2004; Bindlish *et al.*, 2006; Narayan *et al.*, 2004; McCabe *et al.*, 2005; Famiglietti *et al.*, 2008]. Central Iowa is mainly an agricultural region with two major crops, corn and soybean. This experimental site is being used to test retrieval algorithms since agricultural fields are uniform in vegetation type but differ largely in landscape patterns such as soil texture, vegetation conditions, and topography. The 19-day campaign collects wide range of soil and vegetation conditions for soybean and corn fields, thus forms an excellent database to perform spatio-temporal sensitivity analysis of brightness temperature.

2.2.1. Field Measurements

In this study, we selected 4 sampling days (DOY: 178, 182, 186, 188) which best represent the soil moisture wetting and drying cycles under growing vegetation. For our analysis, we used ground measurements of

volumetric soil moisture (VSM), soil temperature, and vegetation water content from the same sampling days (except for 186, when VWC of 187 is used). Two rainfall events were observed in watershed with light showers on DOY: 185, 186, and more significant showers on DOY: 187 elevating SM further. Ground sampling of VWC for corn and soybean noticed a significant increase from DOY: 178–188, with corn mean VWC increasing from 2.9 to 4.5 kg/m², and soybean mean VWC increasing from 0.3 to 0.77 kg/m². Grid board measurements of surface roughness, show a wide range of RMS height (S) and correlation length (L) for corn [S: 0.19–2.55 cm; L: 0.55–26.9 cm] and soybean [S: 0.21–3.05 cm; L: 0–20.8 cm]. These ranges represent the roughness conditions from rolled fields to ploughed surfaces [Alvarez-Mozos *et al.*, 2006; Zhixiong *et al.*, 2005].

2.3. Soil Moisture Active Passive Validation Experiment 2012 (SMAPVEX12)

SMAPVEX12 (Soil Moisture Active Passive Validation Experiment in 2012) was conducted in agricultural region south of Winnipeg, Manitoba (Canada) from 6 June to 17 July 2012. This site is about 15 km × 70 km within the large Red River Watershed. The climate of Winnipeg is classified as extreme humid continental with great difference in summer and winter temperatures. The annual average precipitation is about 52 cm, with most of the precipitation occurring between May to September. Because of the extremely flat topography and substantial snowfall this region is prone to flooding. The watershed is mainly characterized by agricultural land use with a wide range of crop and soil conditions. Soils of this region vary within a distance of few kilometers with heavy clays in the east to loamy sands in the west. The major agricultural crops of the region include cereals, canola, corn, and soybean [Heather *et al.*, 2012 SMAPVEX experimental report]. A total of 55 agricultural sites have been chosen for SMAPVEX12 experiment of which soybean (15), canola (6), corn (10), spring-wheat (14), winter-wheat (2), forage (1), bean (1), and pasture (6). Because of the favorable economic and environmental conditions early in season, more of the soybean fields were planted. Apart from field soil moisture measurements, SMAPVEX12 site is largely monitored with in situ soil moisture stations by United States Department of Agriculture (USDA), Agriculture and Agri-Food Canada (AAFC), and Manitoba Agriculture Food and Rural Initiatives (MAFRI). During SMAPVEX12 field campaign, gravimetric and volumetric soil moisture data were collected almost every alternate day except for rainy days. With the wide range of soil moisture, vegetation and texture conditions observed, SMAPVEX12 site provide an extensive data sets for development and validation of SMAP passive and active soil moisture retrieval algorithms.

2.3.1. Field Measurements

In this study, we use in situ measurements of soil moisture, soil temperature, surface roughness, and vegetation water content collected for soybean and corn fields. Soybean and corn fields show sharp variations in soil texture. Soybean fields show soil texture with sandy loam soils (Field ID: 14, 12, 11, 63, 82, 64, 52) to heavy clay soils (Field ID: 51, 114, 64, 51, 111, 123, 113, 101, 103, 109, 112, 34). Whereas corn fields are mainly sandy (Field ID: 24, 72, 71) and sandy loam (Field ID: 54, 83, 94, 54, 83, 53, 93). For our study, we carefully selected seven (DOY: 159, 164, 169, 174, 181, 190, 199) different wetness days from entire duration of SMAPVEX12 campaign. As mentioned earlier, these wetness days were selected such that they fully represent the wetting and drying cycles of soil moisture under temporally varying vegetation conditions.

2.4. Soil Moisture Retrieval Algorithm

The theory behind microwave radiative transfer model for remote sensing of soil moisture is the large contrast between the dielectric properties of soil (~4) and water (~80). As the amount of water content increases in soil, the dielectric constant increases, while emissivity reduces. The brightness temperature (T_B) of the soil surface is related to its physical effective temperature and emissivity such that:

$$T_{B(\theta,p)} = (1 - R_{(\theta,p)}) \times T_{\text{eff}} = e_{(\theta,p)} \times T_{\text{eff}} \quad (1)$$

where subscript p is the vertical (V) or horizontal (H) polarization and θ denotes incidence angle of the measurement. $R_{(\theta,p)}$ is the p polarized reflectivity from the surface, T_{eff} is the effective soil temperature, $e_{(\theta,p)} = 1 - R_{(\theta,p)}$ is the emissivity of the surface which depends on the dielectric constant (ϵ) of the medium. The dielectric constant (ϵ) of soil is determined by several quantities such as moisture content, bulk density, soil texture composition, soil temperature, and salinity. Of these quantities, ϵ is majorly influenced by soil moisture. The penetration depth δ_p of microwave radiation varies with soil moisture content, such that $\delta_p \sim \lambda$ for volumetric moisture $SM \sim 0.04 \text{ g cm}^{-3}$ (very dry soils) and $\delta_p \sim 0.1 \lambda$ for very wet soils [Ulaby *et al.*, 1986], where λ is the wavelength. Several studies

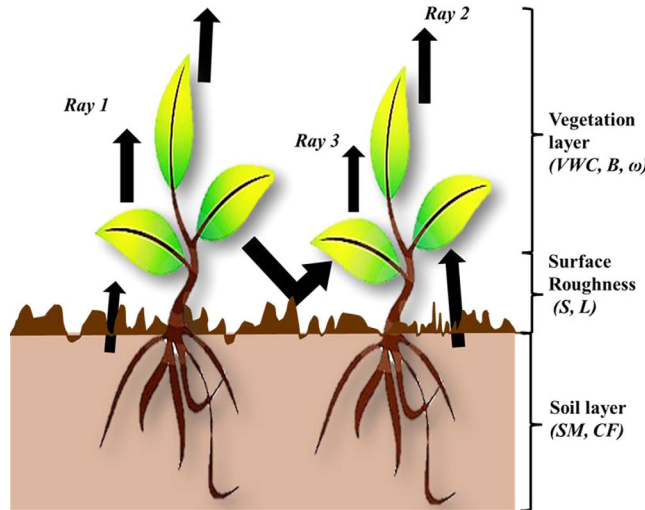


Figure 1. Three layer Zero-Order Radiative Transfer (ZRT) Model, where Ray 1: Soil Emissions Intercepted-Scattered by Vegetation; Ray 2: Vegetation Emission; Ray 3: Soil-Vegetation Reflection/Attenuation, Soil Moisture (SM), Clay Fraction (CF), Surface Roughness RMS height (S), Surface Roughness Correlation Length (L), Vegetation Structure parameter (B), and Scattering Albedo (ω).

[Newton et al., 1982; Schmugge, 1983] relating to sensing depth, have led to the conclusion that soil moisture sensing depth δ_m is on the order of 0.1λ or shallower. Thus, the brightness temperature shows higher sensitivity to the near surface soil moisture variations and reduced sensitivity to deeper layers of soil moisture. Therefore, any nonuniformity in temperature and dielectric constant profiles is significant only for the layer between the surface and the depth of δ_p , because beyond this depth contribution to the brightness temperature (T_B) is very small.

The most widely used radiative transfer model [Mo et al., 1982] under vegetation conditions is

known as τ - ω model described in equation (2).

$$T_{B(p,f,\theta)} = e_{p,\theta} \cdot T_{eff} \cdot \exp\left(-\frac{\tau_{p,f}}{\cos\theta}\right) + T_c \cdot (1 - \omega_{p,f,\theta}) \cdot \left(1 - \exp\left(-\frac{\tau_{p,f}}{\cos\theta}\right)\right) + T_c \cdot \exp\left(-\frac{\tau_{p,f}}{\cos\theta}\right) \cdot (1 - \omega_{p,f,\theta}) \cdot \left(1 - \exp\left(-\frac{\tau_{p,f}}{\cos\theta}\right)\right) \cdot r_{p,f,\theta} \quad (2)$$

where τ_p is the nadir optical depth, ω_p is the single scattering albedo, r_p is the rough surface reflectivity and T_{eff} and T_c are the effective physical temperatures of soil layers and vegetation, respectively. The subscripts, p , θ , and f denote the polarization, angle of incidence, and frequency of measurement. Thus, the total upward microwave emission is a summation of: (Ray 1) upward soil emission attenuated by the vegetation layer through scattering and absorption (τ and ω), (Ray 2) upward emission from vegetation (within vegetation scattering and emission), (Ray 3) vegetation emission reflected by soil (soil surface roughness and reflectivity and attenuated through canopy (Figure 1). Several models [Njoku and Kong, 1977; Wilheit, 1978; Burke et al., 1979] were proposed to determine brightness temperature from nonuniform dielectric and temperature medium. In addition, a comparison between these different models [Schmugge and Choudhury, 1981] led to the conclusion that at longer wavelengths internal reflections between the layered media can be ignored to calculate effective temperature. Thus, for passive remote sensing at L-band ($\lambda \sim 21$ cm, $f \sim 1.4$ GHz), it is reasonable to assume the effective soil temperature to be equal to surface temperature ($T_{eff} \sim TSURF$).

The tau-omega is considered to be Zero-Order Radiative Transfer (ZRT) model, since it ignores multiple scattering within the vegetation layer. These assumptions are considered reasonable during early hours (6 A.M. local time) when soil temperature profile is more uniform and vegetation is in thermal equilibrium with soil ($T_{eff} \sim TSURF \sim T_c$).

Different models [Wang et al., 1983; Choudhury et al., 1979; Wigneron et al., 2011; Lawrence et al., 2013] were proposed to formulate the smooth and rough soil surface reflectivity. The effective rough surface reflectivity in horizontal (H) or vertical (V) polarization is given by

$$R_{rs}^{H,f}(\theta) = [(1 - Q_f) R_s^{H,f}(\theta) + Q_f R_s^{V,f}(\theta)] e^{-G(\theta)h_f} \quad (3a)$$

$$R_{rs}^{V,f}(\theta) = [(1 - Q_f) R_s^{V,f}(\theta) + Q_f R_s^{H,f}(\theta)] e^{-G(\theta)h_f} \quad (3b)$$

where f and θ are frequency and angle of incidence of the measurement. $R_s^{p,f}(\theta)$ are smooth Fresnel reflectivity, Q_f is a polarization mixing factor, h_f is equivalent roughness parameter related to surface RMS height and horizontal correlation length, $G(\theta) = \cos^{n_p}(\theta)$, and n_p is polarization dependent angular exponent. For

model proposed in [Wang *et al.*, 1983] assumes $G(\theta) = 1$ for equations (3a) and (3b), whereas model in [Choudhury *et al.*, 1979] assume $G(\theta) = \cos^2(\theta)$ and $Q_f = 0$. Other empirical models [e.g., Wigneron *et al.*, 2011] developed later consider correlation length to calculate equivalent roughness parameter. Whereas, model proposed in Lawrence *et al.* [2013] allows Q_f and n_p to be calculated from RMS height 'S' and correlation length 'L'. This avoids the assumption of constant values for these parameters and is polarization dependent. In this study we use, roughness model proposed by Lawrence *et al.* [2013].

As mentioned earlier, canopy affects top of the atmosphere brightness temperature (ignoring atmospheric attenuation at L-band) by either radiating its own microwave radiation or absorbing/scattering radiation emanated by the soil. These attenuation effects of vegetation are described by vegetation optical depth $\tau(\lambda, p)$ and single scattering albedo $\omega(\lambda, p, \theta)$ in (2). These factors are dependent on frequency, polarization, incidence angle, vegetation water content, and canopy structure [Mo *et al.*, 1982; Ulaby *et al.*, 1983; Jackson and O'Neill, 1990; Jackson and Schmugge, 1991; Van de Griend and Wigneron, 2004; Wigneron *et al.*, 2011]. The knowledge about the variability of ω_p for H and V polarization are limited [Brunfeldt and Ulaby, 1986]. Van de Griend and Owe [1994] showed the difference between ω_H and ω_V is essentially realized in vegetation exhibiting preferential orientation. The difference, however, is considered to be small, thereby assuming ω_p to be polarization independent.

The single scattering albedo ω accounts for the canopy single volume scattering (Rays 2 and 3, multiple scattering is considered zero) and total extinction properties exhibited by the canopy. It is defined as the ratio of canopy scattering efficiency to the total extinction efficiency (sum of scattering and absorption within canopy) [Mo *et al.*, 1982; Ulaby *et al.*, 1983a]. By fitting model to experimental observations for vegetated fields, several studies [Brunfeldt and Ulaby, 1986; Pampaloni and Paloscia, 1986; Jackson, 1993] have estimated the value of single scattering albedo. The general consensus among these studies indicates that at 1.4 GHz, ω is small and varies from 0.05 to 0.13.

The vegetation optical depth τ_p is related to the vegetation thickness and extinction efficiency of the canopy. The amount of radiation that is not scattered or absorbed by the vegetation is represented by optical depth τ_p , which describes the amount of radiation propagated through vegetation. Since canopy in essence acts as water cloud, τ_p is empirically related [Schmugge *et al.*, 1986; Saleh *et al.*, 2007] to the integrated canopy water content VWC as total mass of water contained in the vertical column of the canopy per unit ground surface area. The canopy architecture, orientation, thickness, and density of vegetation characterize the extinction efficiency of the vegetation. The vegetation optical depth commonly used in soil moisture retrieval algorithms is given by $\tau_p = \text{VWC} \times B$, [Jackson and Schmugge, 1991] where B is a vegetation structure parameter that depends on factors such as frequency, polarization, look angle, and vegetation type. Thus, the vegetation attenuation parameters $\tau_{p,f}$ and $\omega_{f,\theta}$ used in vegetation model are based on the assumptions: (1) at L band, scattering albedo is small and multiple scattering may be ignored, (2) the canopy reflectivity is zero, thus reflection losses at the boundary are not accounted, and (3) due to small refractive index of vegetation layer, soil reflectivity is used in (2) instead of vegetation-soil reflectivity. Several soil moisture retrieval algorithms are developed and validated [Jackson and Le Vine, 1996; Owe *et al.*, 2001; De Jeu and Owe, 2003; Njoku and Chan, 2006; Jones *et al.*, 2011; Santi *et al.*, 2012] based on the above assumptions for soil and vegetation models.

2.5. Global Sensitivity Analysis: Sobol Method

Sensitivity analysis is generally used to identify and quantify the critical inputs (parameters and initial conditions) to a model. Several sensitivity analysis techniques have been developed over time depending on the objective of the study and computational demand. When the input factors are known with little uncertainty, then sensitivity measure is computed by partial derivative of output function with respect to the input factors. This method as mentioned earlier is called local sensitivity analysis (LSA). LSA techniques are best suited for linear systems, since the impact on model output is studied by varying input factors one at a time and very close to the nominal values. On the other hand, land surface models (LSM) or in general any environmental model is rarely additive in nature. Since land surface processes are highly nonlinear and nonmonotonic, thereby exhibiting interactions between the parameters. In such cases, using local SA methods are not suitable for quantitative analysis, since they fail to capture the heterogeneity in input factors. Therefore, techniques such as global sensitivity analysis (GSA) are used, which incorporate variability in the input factors through probability distribution functions using Monte Carlo simulations. Since, Sobol method is capable in handling nonlinear and nonmonotonic functions we use it to analyze our radiative transfer model. We briefly introduce the main concepts of Sobol method here for completeness.

The concept behind variance-based technique is to quantify the amount of variance due to each input factor X_i contributed toward the unconditional variance of the output $V(Y)$. Suppose $Y = f(X)$ is a model function, then Y is the output, $X = (X_1, X_2, X_3, \dots, X_K)$ are K independent input parameters, each one varying over a probability distribution. Applying this configuration to our analysis results in, Y as the output brightness temperature, f as the ZRT model, and X_K as the input parameter vector with $K = 8$, and $[X_1, X_2, X_3, X_4, X_5, X_6, X_7, X_8]$ as [Soil Moisture (SM), Clay Fraction (CF), Surface Roughness- RMS height (S), Surface Roughness-Correlation length (L), Surface Temperature (TSURF), Vegetation Water Content (VWC), Vegetation Structure (B), Scattering Albedo (ω)].

Sobol suggested that the function f can be decomposed into summands of increasing dimensionality;

$$f(X_1, X_2, \dots, X_K) = f_0 + \sum_i f_i(X_i) + \sum_{i < j} f_{ij}(X_i, X_j) + \dots + f_{1\dots K}(X_1, \dots, X_K) \quad (4)$$

If each term in the above equation is square integrable with average zero and input parameters are not dependent, then f_0 is a constant and is equal to the expectation value of the output and summands are mutually orthogonal. Additionally, this decomposition is unique. With the assumption that the parameters are mutually orthogonal, the total unconditional variance is [Saltelli et al., 2008];

$$V_T = \sum_i V_i + \sum_{i < j} V_{ij} + \dots + \sum V_{1,2,3, \dots, K} \quad (5)$$

$$V_i = V[E(Y|X_i)]; \quad V_{ij} = V[E(Y|X_i, X_j)] - V_i - V_j \quad (6)$$

where $V[E(Y|X_i)]$ is the expected amount of variance that would be removed if the true value of X_i is learnt, $V_{ij} = V[E(Y|X_i, X_j)]$ describes the joint effect of pair (X_i, X_j) and is called second-order effect thus measuring the variance contributed by this interaction to total model variance, similarly higher order effects can be computed.

GSA ranks the input parameters based on the amount of variance that would disappear on learning the true value of x^* . For a nonlinear model, the total output variance is decomposed into variances caused due to first (fractional variance of X_i to output) and higher order (variance caused due to interactions between the factors, $X_{ij}, i \neq j$).

Using first and other order variances, sensitivities indices S_i are calculated by dividing $V[E(Y|X_i)]$ with total variance V_T .

$$\text{First-Order Sensitivity Measure : } S_i = \frac{V_i}{V_T}; \quad (7)$$

$$\text{Second-Order Sensitivity Measure : } S_{ij} = \frac{V_{ij}}{V_T}; \quad (8)$$

$$\text{Total } S_{T_i} = S_i + \sum_{j \neq i} S_{ij} + \dots \quad (9)$$

where S_i is the first-order sensitivity index for factor X_i , which measures variance contribution of parameter X_i on total model variance, S_{ij} is the second-order sensitivity index signifying the interactions between parameters i and j , and S_{T_i} is sum of main effects and all their interactions with the other parameters (up to k th order). The calculation of S_{T_i} can be based on $E[V(Y|X_{-i})]$, variation of all parameters except X_i ;

$$S_{T_i} = \frac{E[V(Y|X_{-i})]}{V(Y)}. \quad (10)$$

For additive models, S_i and S_{T_i} are equal and sum of S_i (and thus S_{T_i}) is 1. For nonlinear models (or nonadditive models) S_{T_i} is greater than S_i and $\sum S_i < 1$ ($\sum S_{T_i} > 1$). The difference between S_{T_i} and S_i is used to analyze the interactions between parameter X_i and the other parameters.

2.6. Evaluation of the Parameters Using Sensitivity Analysis

A high value of S_i implies X_i as significant parameter in influencing the output and should be given priority in estimation. Whereas a low value of S_{T_i} indicates that the parameter is not important either singularly or via interactions, and can be frozen to its optimal value (parameter fixing).

Table 1. Parameter Ranges of Corn and Soybean SMAPVEX12 Fields for Selected Sampling Days

| Parameters SMAPVEX12 | Crop Type | DOY 159 | DOY 164 | DOY 169 | DOY 174 | DOY 181 | DOY 190 | DOY 199 |
|---|-----------|-----------|-----------|-----------|-----------|-----------|-----------|-----------|
| Soil moisture (SM) (V/V) | Corn | 0.02–0.34 | 0.07–0.46 | 0.1–0.45 | 0.05–0.37 | 0.012–0.3 | 0.03–0.43 | 0.03–0.38 |
| | Soybean | 0.04–0.47 | 0.12–0.57 | 0.06–0.52 | 0.08–0.59 | 0.04–0.41 | 0.04–0.45 | 0.05–0.40 |
| Clay fraction (CF) (%) | Corn | | | | 5%–38% | | | |
| | Soybean | | | | 4.5%–66% | | | |
| RMS height (S) (cm) | Corn | | | | 0.3–1.7 | | | |
| | Soybean | | | | 0.2–2.0 | | | |
| Correlation length (L) (cm) | Corn | | | | 4.5–23 | | | |
| | Soybean | | | | 5–23 | | | |
| Surface Temp (TSURF) (Kelvin, K) | Corn | 293–300 | 281–294 | 288–293 | 287–295 | 292–298 | 291–300 | 291–296 |
| | Soybean | 292–302 | 281–292 | 287–293 | 286–292 | 290–298 | 292–299 | 292–299 |
| Vegetation Water Content (VWC) (Kg/m ²) | Corn | No veg | 0.01–0.1 | 0.1–0.39 | 0.15–0.45 | 0.5–1.5 | 1.7–2.4 | 2.2–4.22 |
| | Soybean | No veg | 0.03–0.13 | 0.04–0.25 | 0.05–0.29 | 0.05–0.52 | 0.08–0.7 | 0.17–2.7 |
| Vegetation Structure (B) | Corn | | | | 0.1–0.15 | | | |
| | Soybean | | | | 0.05–0.1 | | | |
| Scattering Albedo (ω) | Corn | | | | 0–0.05 | | | |
| | Soybean | | | | | | | |

We analyzed a time series Global Sensitivity Analysis (GSA) of Zero-Order Radiative Transfer (ZRT) Model to input parameters. The analysis was conducted for each of the 4 days in SMEX02 fields and for 7 days in SMAPVEX12 fields. The field observations of SMEX02 and SMAPVEX12 are significantly different with respect to soil moisture, soil texture, soil temperature, surface roughness, and vegetation water content. In this study, it is assumed that the field observations are true representative of variability that is observed. In our analysis, we assume uniform distribution for all parameters to effectively capture the heterogeneity observed in the fields. Field observations are used to represent maximum (max) and minimum (min) values. Tables 1 and 2 show observed soil and vegetation parameter ranges for SMAPVEX12 and SMEX02. Due to irregular planting periods, not all fields of corn (or soybean) showed similar growth trend, and not all fields were sampled on all sampling days, which has resulted in irregular ranges for VWC. Since we want to study the influence of growing vegetation, we used highest observed VWC values than previous sampling day. It is assumed that parameters such as Clay Fraction (CF), Surface Roughness RMS height (S), Surface Roughness Correlation Length (L), Vegetation Structure (B) and Scattering albedo (ω) are static during our analysis period, and same range is considered for all sampling days. Since, there were no major agricultural practices performed during the growing cycle, our assumption of similar surface roughness conditions on all days holds valid.

To estimate first-order and total sensitivity indices S_i , and S_{Ti} for k parameters with N sample size requires $N(k + 2)$ model evaluations, i.e., for $K = 8$ parameters and $N = 30,000$ sample size, a total of 300,000 model evaluations were performed. While computing Sobol indices, we employ Sobol quasi random sampling instead of standard Monte Carlo sampling schemes. To avoid lumped sampling or clustering, quasi random sampling adds samples to the sequence away from the earlier sampled points and fills the unit hypercube

Table 2. Parameter Ranges of Corn and Soybean SMEX02 Fields for Selected Sampling Days

| Parameters SMEX02 | Crop Type | DOY 178 | DOY 182 | DOY 186 | DOY 188 |
|---|-----------|---------------|---------------|--------------|---------------|
| Soil moisture (SM) (V/V) | Corn | 0.07–0.16 | 0.05–0.15 | 0.06–0.27 | 0.11–0.37 |
| | Soybean | 0.07–0.16 | 0.04–0.14 | 0.05–0.23 | 0.1–0.29 |
| Clay fraction (CF) (%) | Corn | | | 10%–40% | |
| | Soybean | | | 10%–40% | |
| RMS height (S) (cm) | Corn | | | 0.19–2.5 | |
| | Soybean | | | 0.21–3.05 | |
| Correlation length (L) (cm) | Corn | | | 0.56–26.9 | |
| | Soybean | | | 0.43–20.80 | |
| Surface Temperature (TSURF) (Kelvin, K) | Corn | 296.15–318.5 | 299–310 | 296.15–304.5 | 295.85–299 |
| | Soybean | 296.15–320.65 | 300.15–312.55 | 297.4–310.75 | 294.65–309.65 |
| Vegetation Water Content (VWC) (Kg/m ²) | Corn | 1.97–4.27 | 2.25–5.23 | 3–6 | 3.5–6.05 |
| | Soybean | 0.2–0.47 | 0.27–0.66 | 0.32–0.69 | 0.4–1.43 |
| Vegetation Structure (B) | Corn | | | 0.1–0.15 | |
| | Soybean | | | 0.05–0.1 | |
| Scattering Albedo (ω) | Corn | | | 0–0.05 | |
| | Soybean | | | | |

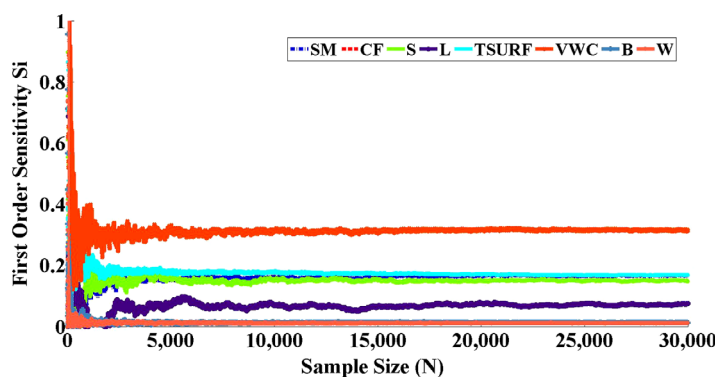


Figure 2. Evolution of first-order sensitivity index for Soil Moisture (SM), Clay fraction (CF), RMS height (S), Correlation length (L), Surface Temperature (TSURF), Vegetation Water Content (VWC), Vegetation structure parameter (B), Scattering Albedo (ω).

samples used for the model evaluations were sampled 1000 times with replacement, and sensitivity indices were calculated each time. The 95% confidence intervals were then constructed on the distributions obtained for S_i 's and S_{T_i} 's using percentile method.

3. Results and Discussions

We analyzed our results at $N = 30,000$, where the sensitivity indices were found to be stabilized Figure 2. The first-order and total sensitivity indices are calculated along with their 95% confidence intervals which are obtained through bootstrapping. In the following sections, we present and discuss the Sobol sensitivity indices for each parameter for SMAPVEX12 and SMEX02. We also discuss the sensitivity of brightness temperature to soil-vegetation parameters in increasing SM ranges (for stepwise increment of 0.05 V/V increment in SM) while retaining other parameters to their observed ranges for selected days, Figures 7a–7e. Though SMAPVEX12 and SMEX02 are climatically similar regions, they exhibited varied field conditions.

3.1. First-Order Sensitivity Measures

3.1.1. Soil Moisture (SM)

In general, brightness temperature showed higher sensitivity to SM in SMAPVEX12 than in SMEX02 due to wider SM ranges observed in case of SMAPVEX12 fields. A clear temporal variability in SM sensitivity due to wetting and drying cycle can be seen in both the fields. We notice an unfamiliar behavior of brightness temperature sensitivity to SM in the presence of vegetation Figures 3–6. The brightness temperature sensitivity to SM does not increase linearly with increase in SM. For example, DOY: 164, 169 show high SM (max: 0.45 V/V) observed in corn fields for SMAPVEX12, however, this increase in SM is not reflected in increased sensitivity of brightness temperature to SM. Similarly DOY: 188 (corn) during SMEX02 was wettest day and high VWC when compared to previous sampling days, however, we notice a decrease in sensitivity to SM and VWC, but sensitivity to B, S, and L parameters and their interactions has increased. We will discuss the behavior of B, S, L parameters and their interactions in their respective sections. To analyze this behavior of decrease in SM sensitivity with increase in SM further, we calculated sensitivity indices for 0.05 V/V range in SM for selected days Figures 7a–7f. Soil moisture shows a decreasing exponential function ($R^2 \sim 0.99$) with very low sensitivity from 0.2 V/V onward. Soil water in the range of 0.01–0.1 V/V are tightly bound by adhesion forces to soil particles, thereby exhibiting emissivities which are close to that of dry soil (0.95), but with increase in SM the unbound water also called as “free water” increases thus reducing emissivities steeply to 0.6 for SM 0.2 V/V. This is because after a certain SM value (transition soil moisture) any further increase in SM does not influence emissivity significantly [Schmugge *et al.*, 1974]. However, the transition soil moisture changes with soil texture, being higher for more clayey soils. SM shows higher sensitivity in lower clay soils with steep decrease in SM sensitivity with increase in SM ranges, whereas in higher clay soils the SM sensitivities are small and decreases less steeply Figures 7c and 7d. The increased dominance of texture in higher clay soils and higher sensitivity to vegetation and roughness effects with increasing SM is also a reason for low SM sensitivity Figures 7a–7f.

uniformly. Also, quasi random sampling results in faster convergence rate of $1/N$ as compared to $1/\sqrt{N}$, which is necessary to reduce computational demands.

2.6.1. Bootstrapping

In order to build confidence intervals for the first-order and total Sobol sensitivity indices, we use bootstrap technique with resampling [Efron and Tibshirani, 1994], since it is computationally very demanding to repeat $N(k + 2)$ model runs several times. The N samples used for the model evaluations were sampled 1000 times with replacement, and sensitivity indices were calculated each time. The 95% confidence intervals were then constructed on the distributions obtained for S_i 's and S_{T_i} 's using percentile method.

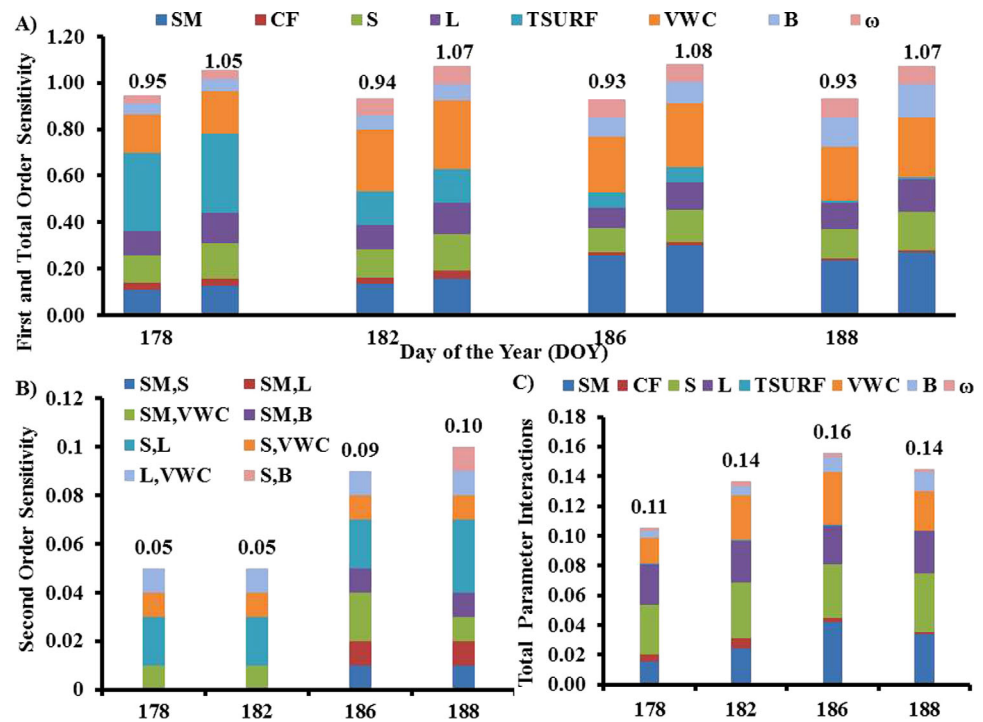


Figure 3. SMEX02 Corn Fields (a) First-Order Sensitivity S_i (left) and Total Sensitivity S_{Ti} (right), (b) Second-Order Sensitivity S_{ij} , and (c) Total Parameter Interactions for DOY: 178, 182, 186, 188. Sum of sensitivity indices are mentioned on top of bars.

3.1.2. Clay Fraction (CF)

Compared to other parameters, brightness temperature shows consistently small sensitivity to CF in field condition for both SMAPVEX12 and SMEX02 when compared to other parameters. Higher CF sensitivities are realized in soybean fields in SMAPVEX12 due to higher CF% observed. As expected, CF signature is more visible in bare and dry conditions DOY: 178, 182 (SMEX02). Analyzing the CF sensitivity for increasing SM ranges, it is noticed that CF shows a decreasing sensitivity function with high sensitivities noticed up to 0.15–0.2 V/V for higher clay soils (soybean field in SMAPVEX12) and up to 0.1–0.15 V/V for lower clay soils (corn fields in SMAPVEX12 and SMEX02) after which it decreases steeply. Soil texture is important, since it determines surface area, size, and shape of the soil particles thereby influencing the amount of bound and free soil water. Therefore, clay fraction (CF) of soils largely determines the transition soil moisture, i.e., the SM range beyond which the adhesion forces of CF largely weaken. Thus, sensitivity of CF up to transition SM is high since it determines surface area for bound water. Beyond the transition SM, influence of CF through adhesion forces reduces since proportion of unbound water increases, thereby reducing the effect of CF. As this transition SM is higher in higher clay soils (SMAPVEX12), we notice high sensitivity to CF up to SM range of 0.15–0.2 V/V.

3.1.3. Surface Roughness (S and L)

In general, significant surface roughness effects are noticed in SMEX02 fields than SMAPVEX12. For similar surface roughness, brightness temperature shows higher sensitivity to roughness parameters (S and L) on wet days (SMAPVEX12 DOY: 164, 169 and SMEX02 DOY: 188) than on dry days. Analyzing the sensitivity of brightness temperature to RMS height “S” and correlation length “L” with SM ranges, resulted in an increasing sensitivity function for S and L with increasing SM. As expected sensitivity indices of RMS height “S” is higher than “L.” But surface roughness parameters (S and L) show different sensitivity functions to SM and soil texture Figures 7a–7f. We notice a linear sensitivity function in case of higher clay soils ($R^2 \sim 0.97$; CF 0.05–0.66, soybean in SMAPVEX12) and a logarithmic function in case of lower clay ($R^2 \sim 0.94$; CF 0.05–0.38, corn in SMAPVEX12) best fit the analysis. In case of soybean fields (SMAPVEX12, high clay soil), S overrides SM and CF sensitivity curves around 0.05–0.1 V/V and 0.25–0.3 V/V, respectively, whereas in case of corn fields (SMAPVEX12, low clay soil) S overrides SM and CF sensitivity around 0.1–0.15 V/V (Figures 7c and 7d). Thus, the roughness observed before S overriding L sensitivity could be accounted due to dielectric

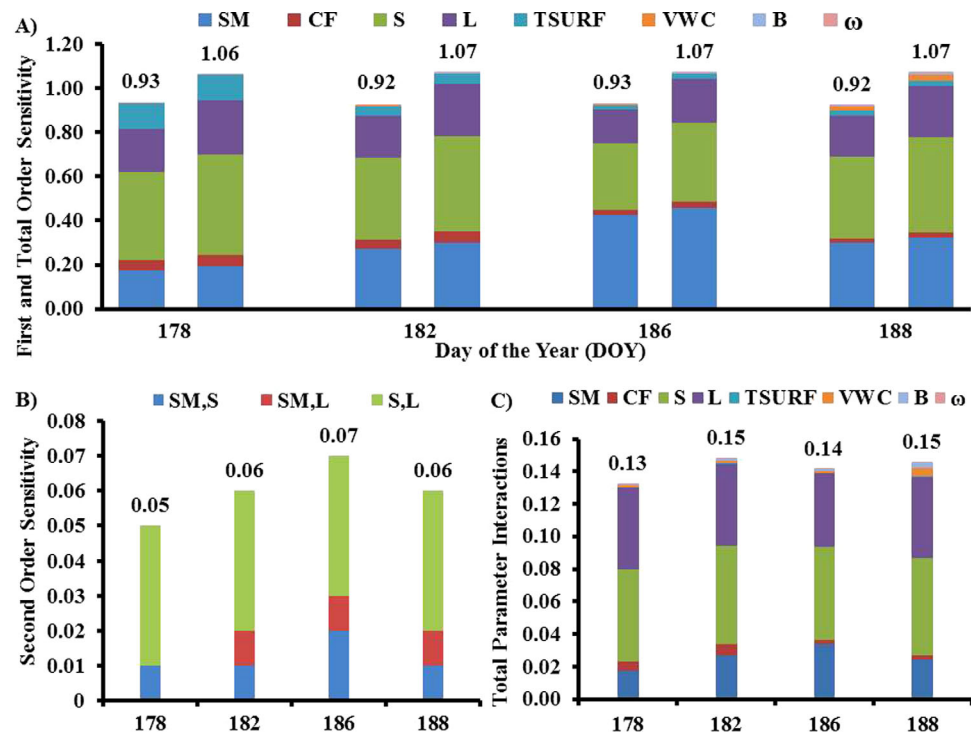


Figure 4. SMEX02 Soybean Fields (a) First-Order Sensitivity S_i (left) and Total Sensitivity S_{Ti} (right), (b) Second-Order Sensitivity S_{ij} , and (c) Total Parameter Interactions for DOY: 178, 182, 186, 188. Sum of sensitivity indices are mentioned on top of bars.

volume scattering in soils whereas after which roughness effects are contributed mainly due to surface contributions (S and L). With further increase in SM, spatial variability of SM in horizontal direction due to lateral conductivity starts to dominate. This is clearly noticed with correlation length (L) overriding SM and CF sensitivity at 0.2–0.25 V/V and 0.35–0.4 V/V, respectively, in soybean (SMAPVEX12, high clay soil), whereas in case of corn (SMAPVEX12, low clay soil) L overrides SM and CF sensitivity around 0.2–0.25 V/V (Figures 7c and 7d). However, in SMEX02 due to high roughness conditions and low CF range, S and L overrides SM at all moisture conditions (Figures 7a and 7b). Chauhan [2002] also found that surface roughness gain more impact in wetter conditions. Our results are also supported by Wigneron *et al.* [2001], who proposed surface roughness may be a contribution of dielectric roughness and physical roughness. According to Panciera *et al.* [2009] higher roughness conditions are observed in clayey soils than sandy soils due to higher moisture heterogeneity exhibited by clayey soils.

3.1.4. Surface Temperature (TSURF)

Sensitivity of brightness temperature (TB) to surface temperature effects are much less realized in SMAPVEX12 fields but shows significant effect on dry days of SMEX02 fields (DOY: 178, 182) (Figures 3a and 4a), due to wide and higher ranges of TSURF observed in SMEX02. Also, TSURF shows a decreasing sensitivity function with increasing SM. TSURF does not participate in any second-order interactions with other parameters. For any TSURF range, brightness temperature it show higher sensitivity to TSURF at lower SM ranges and sensitivity gradually decreases with increasing SM.

3.1.5. Vegetation Water Content (VWC)

Sensitivities of VWC exhibits clear spatio-temporal variation, with higher interactions observed on higher VWC and wet days. Consider DOY: 186, 188 (SMEX02) and DOY: 190 (SMAPVEX12), where increase in VWC has not resulted in its proportionate increase in TB sensitivity to VWC. Growing canopy will not only attenuate/scatter soil emissions (Ray 1 in Figure 1) but also attenuate/scatter the reflected vegetation emission (Ray 3 in Figure 1), acting as its own and soil emission attenuator. This explains the phenomenon of reduced sensitivity to VWC, increasing sensitivity to B parameter and increased interactions with increasing VWC. Due to wider and higher VWC ranges observed in SMEX02 fields, high first-order sensitivities are observed in SMEX02 than in SMAPVEX12 (Figures 3–6). The first-order sensitivity of VWC remains similar with

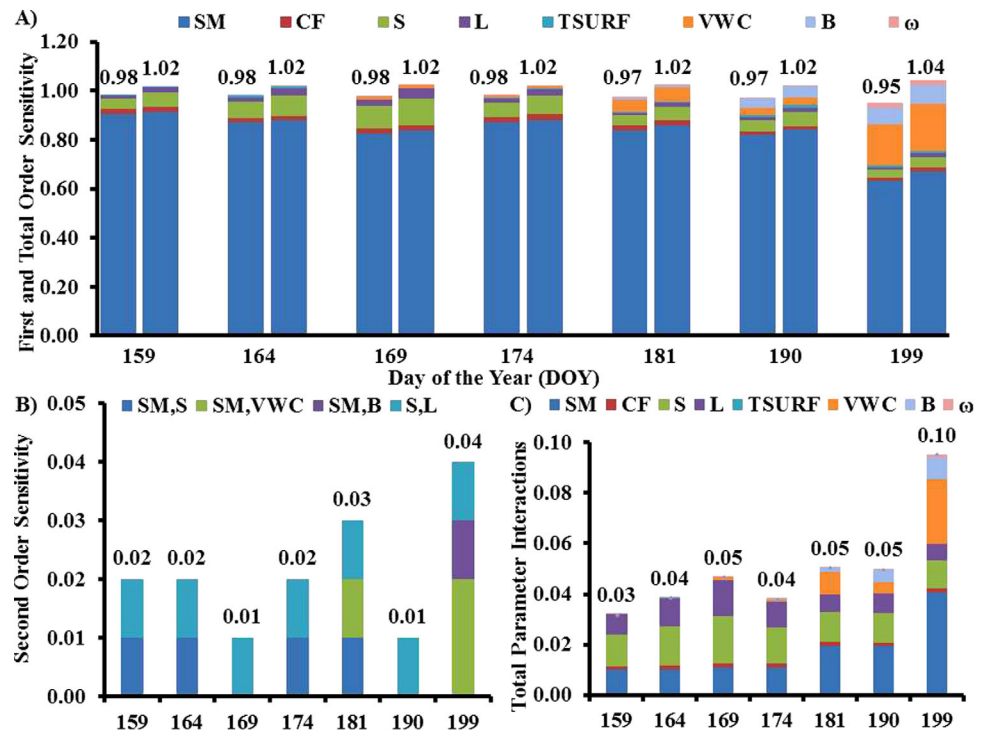


Figure 5. SMAPVEX12 Corn fields (a) First-Order Sensitivity S_i (left) and Total Sensitivity S_{Ti} (right), (b) Second-Order Sensitivity S_{ij} , and (c) Total Parameter Interactions for DOY: 159, 164, 169, 174, 181, 190, 199. Sum of sensitivity indices are mentioned on top of bars.

observed VWC ranges irrespective of other field conditions, however, with different higher order interactions, e.g., SMEX02 (DOY: 178) and SMAPVEX12 (DOY: 199). A significant contribution from VWC is realized in case of corn plants on all days of SMEX02 and SMAPVEX12 (DOY: 181–199). Also, an increasing sensitivity function for VWC at higher SM ranges is observed (Figures 7a, 7e, and 7f). Vegetation shows an exponential growth in the SMAPVEX12 fields where significant VWC is noticed on last three sampling days of SMAPVEX12. The increased sensitivity to VWC for soybean on DOY: 199, when mean (VWC) > 1 kg/m² is observed, which otherwise is not noticed on other sampling days of SMAPVEX12.

3.1.6. Vegetation Structure (B)

Corn fields show more sensitivity to B parameter than soybean fields, due to the definite vertical structure of corn plants (Figure 3) which is otherwise hardly noticed in soybean plants. The B parameter shows a gradual increase in its sensitivity with growing VWC and increasing SM. These results agree with Seo *et al.* [2010], where B parameter shows highest sensitivity in wet soils and VWC > 1 kg/m². Since, with growing vegetation there is a progressive change in canopy structure, i.e., length, thickness and size of leaves, stalks, etc. This changing canopy structure also modifies soil radiation through scattering and adds its own emissions, resulting in soil and vegetation interactions as discussed below. The first-order effects are realized for corn on all sampling days (SMEX02) and DOY: 190, 199 (SMAPVEX12). We clearly notice the interception/scattering of soil radiations by B through (SM, B) for grown corn plants which otherwise not seen in soybean. Also, an increasing sensitivity function of B with SM is observed (Figures 7a, 7e, and 7f).

3.1.7. Single Scattering Albedo (ω)

Similar to B parameter, brightness temperature shows primarily no sensitivity to albedo in soybean plants but its influence is realized in structured vegetation such as corn, similar to Chauhan [2002]. Like VWC and B, albedo also shows increasing sensitivity with growing vegetation. The scattering albedo (ω) does not participate in any higher order interactions, however, this might not be the case at higher albedo values which are common in bushy, structured vegetation, and forests. However unlike VWC and B, albedo shows a decreasing sensitivity with increasing SM. Thus, assuming a constant look-up table for albedo and B under all SM conditions, VWC, and vegetation types will compromise SM retrieval accuracy. Because B and albedo

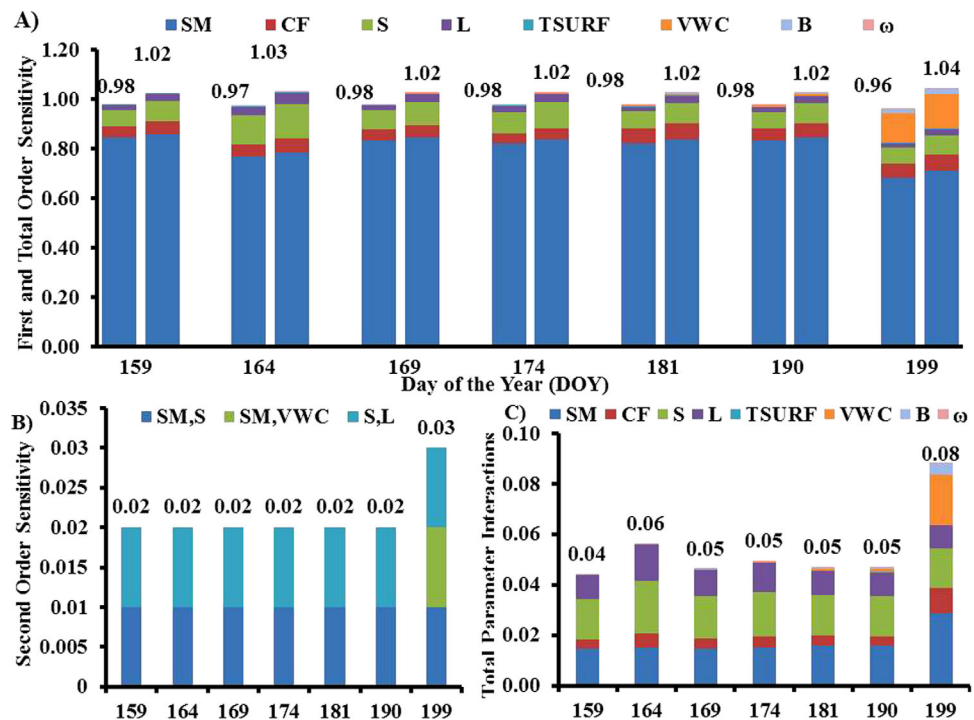


Figure 6. SMAPVEX12 Soybean fields, (a) First-Order Sensitivity S_i (left) and Total Sensitivity S_{Ti} (right), (b) Second-Order Sensitivity S_{ij} , and (c) Total Parameter Interactions for DOY: 159, 164, 169, 174, 181, 190, 199. Sum of sensitivity indices are mentioned on top of bars.

(ω) show increasing sensitivity with growing vegetation, a combined parameter dependent on VWC can be developed.

3.2. Second-Order Interactions

SMEX02 fields show more of higher order interactions than SMAPVEX12 fields. In the following discussion, an overview of total interactions and second-order interactions are presented. In past environmental studies using GSA, interactions are sufficiently captured by second-order interactions, however, in this study we notice interactions greater than second order are also present. The total interactions exhibited by the parameter can be obtained from the difference between its total and first-order measures as discussed below.

3.2.1. Interactions of Soil Moisture (SM, VWC), (SM, B), (SM, S), and (SM, L)

It is understood that, the upward soil emission contributing to the brightness temperature is interrupted by vegetation, thus determining the amount of soil radiation passing through canopy. Interactions of soil parameters with vegetation parameters such as vegetation water content (VWC) and vegetation structure (B) are reflected through interactions between (SM, VWC) and (SM, B). Due to the definite structure and significant VWC observed in corn, a consistent (SM, VWC) interactions are seen on all sampling days in corn (SMEX02) and on DOY: 181, 190, 199 (SMAPVEX12), clearly displaying the shielding effect of grown canopy which are otherwise not observed in early stages of corn growth in SMAPVEX12 and soybean. Apart from VWC, vegetation structure (geometry, orientation, thickness, etc.) also play a significant role in screening/scattering soil emissions and interception of rainwater, displaying an interaction of (SM, B) on DOY: 186, 188 (SMEX02) and DOY: 199 (SMAPVEX12). An increase in SM on DOY: 186, 188 did not result in increased (SM, VWC) interactions, but produced interactions between surface-roughness and vegetation as discussed below. The scattering of soil moisture emission by surface roughness parameters (S and L) can be realized through interactions between (SM, S) and (SM, L). The scattering of soil radiations by RMS height (S) is realized on all sampling days except on DOY: 178, 182 for corn (SMEX02) due to low SM and high VWC. Further, the interactions between (SM, L) are realized only on higher SM conditions and smaller L values SMEX02 fields (DOY: 182–188). This is because the connectivity of soil water flow in horizontal direction starts to influence only at higher SM conditions.

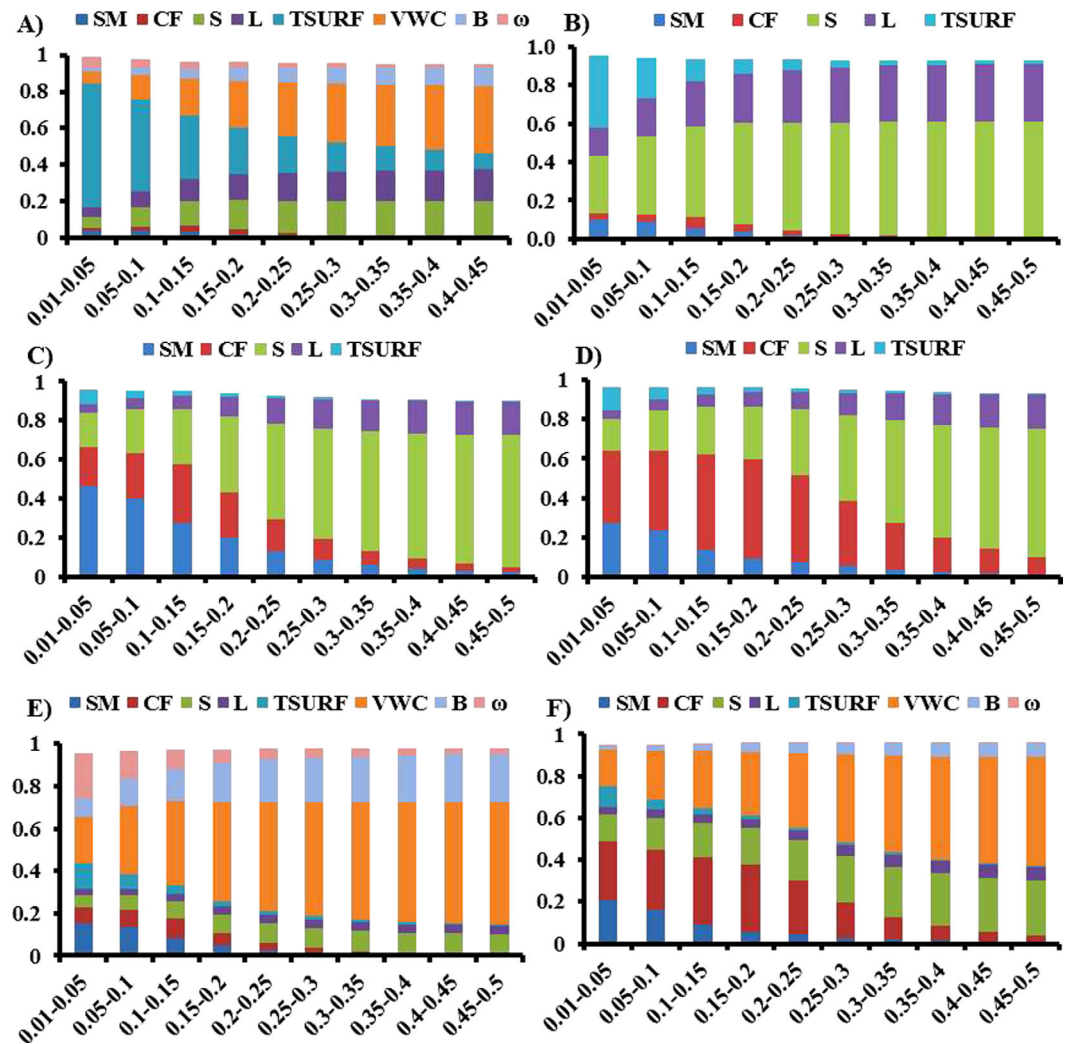


Figure 7. First-Order Sensitivities of Parameters (S_1) on Y-axis and Soil Moisture (SM) ranges on X-axis. (a) SMEX02 Corn DOY: 178, (b) SMEX02 Soybean DOY: 178, (c) SMAPVEX12 Corn DOY: 159, (d) SMAPVEX12 Soybean DOY: 159, (e) SMAPVEX12 Corn DOY: 199, and (f) SMAPVEX12 Soybean DOY: 199.

The correlation lengths (L) which is the periodicity of soil surface, will then define soil water flow thereby displaying (SM, L) interactions. However, the consistent high SM in SMAPVEX12 has not resulted in similar (SM, L) interactions. Thus, there could be a range of SM and above which the (SM, L) interactions are undermined due to higher SM. Whereas the (SM, S) are expected in all conditions due to the scattering influence of random roughness (S) on soil emissions. This can also be realized through Figures 7a–7f where increase in SM, resulted in increased sensitivity of brightness temperature to surface roughness (S and L) parameters increases.

3.2.2. Interactions of Surface Roughness (S, L), (S, VWC), (S, B), and (L, VWC)

The vegetation emission reflected by rough surface is represented by Ray 3 (Figure 1) is captured through interactions between (S, B), (S, VWC), and (L, VWC). These interactions are noticed only in corn (SMEX02) and not in soybean (SMEX02), due to prominent vegetation structure and higher VWC observed in corn plants. However, none of these interactions are observed in SMAPVEX12 fields due to smaller VWC and milder surface roughness conditions compared to SMEX02 fields. Therefore, we can expect to see higher interactions between surface roughness and vegetation parameters (higher contribution from Ray 3) in fields with higher surface roughness, and structured plants with significant VWC. Also, a consistent (S, L) interaction is realized on all sampling days in SMEX02 and SMAPVEX12 fields emphasizing their underlying correlation.

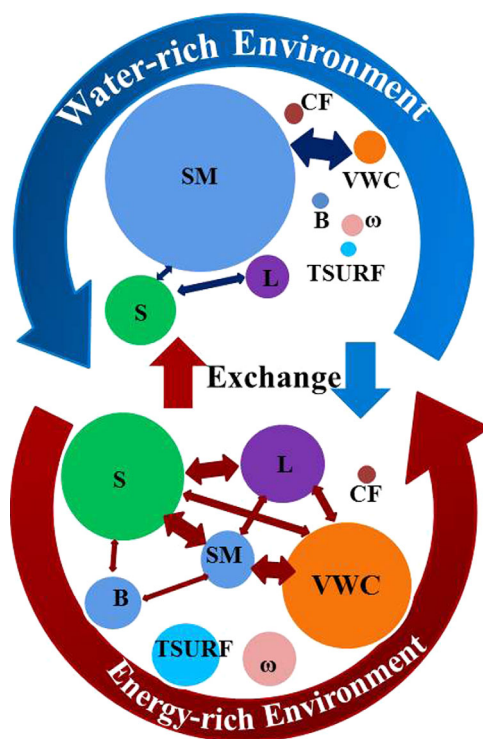


Figure 8. Proposed conceptual diagram, where interactions observed in the Energy rich environments are different and higher than those observed in Water rich environments. Different parameters are represented by different where parameter's contribution is represented by circle size and parameter interaction by the arrow thickness.

3.3. Total Interactions, Linearity, and Nonlinearity

For additive models, since there are no parameter interactions first-order (S_i) and total order (ST_i) sensitivity indices are equal ($S_i = ST_i$) and sum to 1 [Saltellii et al., 2004]. We observe higher order interactions in higher VWC and SM conditions. In SMAPVEX12 fields, ZRT model is nearly linear with nonlinearity increasing with growing canopy, displaying second-order interactions of $\sim 2\%$ seen on all sampling days, and increasing up to $\sim 4\%$ at the end of field campaign Figures 5b and 6b. And, total interactions of $\sim 5\%$ are seen on almost all days but increases up to $\sim 10\%$ on DOY: 199 in SMAPVEX12 fields (Figures 5c and 6c). In case of SMEX02 fields, ZRT model is more nonlinear with second-order interactions increasing from 5 to 10%, in corn and up to 7% in soybean, with total interactions of $\sim 15\%$ because of higher VWC and roughness conditions. In case of corn fields, first-order effects are contributed by vegetation whereas in soybean fields first-order effects are contributed by roughness conditions, which are otherwise shielded by corn plants and displayed through second-order interactions (Figure 3b).

4. Conclusions

GSA method is particularly useful to analyze nonlinear models with higher order interactions. Using GSA for Zero-Order Radiative Transfer (ZRT) model resulted in primarily four parameters (SM, VWC, S, and L) in SMEX02 region and one parameter (SM) in SMAPVEX12 region to be sensitive to brightness temperature, with sensitivities showing a temporal variation. Also, parameter interactions increased with VWC and roughness conditions. The soil-vegetation interactions are realized through (SM, VWC), (SM, B), (S, VWC), (L, VWC), (S, B), (SM, L), and (SM, S). A clear distinction between the similar influence of surface roughness and vegetation parameters are achieved, along with spatio-temporally varying parameter interactions which enhanced our understanding of ZRT and will improve soil moisture retrievals. Based on our analysis of GSA for ZRT model under different spatio-temporal conditions, we have proposed a conceptual model Figure 8. Considering the SMAPVEX12 fields to be water rich environment (due to higher observed SM) and SMEX02 fields to be energy rich environment (due to lower SM and wide ranges of TSURF), our results indicate that first-order effects of parameters changes with water and energy rich environments. Particularly, parameter interactions were observed to be higher and diverse in energy rich environments (SMEX02) than water rich environments (SMAPVEX12). Even under the similar vegetation effects, DOY: 199 (SMAPVEX12) and DOY: 168 (SMEX02) we observe reduced parameter interactions in water rich fields (SMAPVEX12) than SMEX02 fields. The conceptual model in Figure 8 represents the water-rich and energy-rich environments with different parameter significance and interactions. The brightness temperature (TB) in energy rich environment is more sensitive to parameters such as S, L, TSURF, VWC, B, and their interactions, whereas for water-rich environments we tend to observe TB highly sensitive to SM and low parameter interactions. The transition between these two environments occurs through exchange of energy and water with either increase or decrease of land-surface interactions. This analysis is particularly relevant for recently launched Soil Moisture Active Passive (SMAP) mission for improved theoretical developments in radiative transfer models under highly heterogeneous landscapes and different hydro-climates. Accounting for the higher order interactions in the soil moisture retrieval algorithm will significantly improve accuracy of soil moisture product. Nonetheless this

is challenging task since the sensitivity of many parameters are not time stable, but vary with wetness and vegetation conditions.

Future scope of this work can include developing hydro-climate specific soil moisture retrieval algorithm. Also the sensitivity of B parameters changes with vegetation water content, thus developing a combined vegetation parameter is very relevant. This will avoid using constant look up tables for B parameter. This analysis can also be extended in developing a unified soil moisture map using different satellites (SMOS, SMAP), sensors (active/passive), and frequencies (L, C, X).

In summary:

1. Attenuation of soil emission by vegetation parameters (VWC, B) can be significant in structured plants (corn). And, interactions appear to increase with roughness and SM conditions.
2. The effects of B and albedo are not realized in soybean plants but show significant contribution in structured vegetation such as corn plants. These parameters show increasing sensitivity with increasing VWC and SM. Thus, assuming a constant value of B under all SM and VWC conditions will affect soil moisture retrieval accuracy.
3. For similar surface roughness conditions, sensitivity to roughness parameters is higher in wet soils than dry soils. Because of only skin depth emission in case of moist soils, radiations are more perturbed due to surface roughness in wet soils than in dry soils.
4. SM and TSURF show a monotonically decreasing sensitivity function, whereas VWC, S, L, and B show a monotonically increasing sensitivity function with increase in SM. CF sensitivity shows an increasing function up to the transition SM, after which it drops exponentially with increase in SM. This peak observed at the transition SM changes with the percentage of clay fraction.
5. Pixels with soil moisture below the transition soil moisture (which is variable with clay content) prove to show high sensitivity to brightness temperature (TB). This sensitivity decreases exponentially with increase in soil moisture due to increasing sensitivity of other soil and vegetation parameters. Thus, soil moisture retrieval accuracy degrades with increasing wetness if effects of soil-vegetation parameters are not accurately accounted.

Acknowledgments

We acknowledge the funding support of NASA THPs (NNX08AF55G and NNX09AK73G) and NSF (DMS-09-34837) grants. The data for SMEX02 and SMAPVEX12 field campaign are available at NSIDC's <http://nsidc.org/data/smap/validation/val-data.html> and http://nsidc.org/data/amr_validation/soil_moisture/smex02/index.html. The data sets downloaded are ground soil moisture, soil temperature, soil texture, vegetation water content, and surface roughness. We would like to thank anonymous reviewers for their insightful comments in improving the manuscript and Vadose Zone Research Group (VZRG) for their support and guidance.

References

- Alvarez-Mozos, J., J. Casali, M. González-Audicana, and N. E. Verhoest (2006), Assessment of the operational applicability of RADARSAT-1 data for surface soil moisture estimation, *IEEE Trans. Geosci. Remote Sens.*, *44*(4), 913–924.
- Bindlish, R., T. J. Jackson, A. J. Gasiewski, M. Klein, and E. G. Njoku (2006), Soil moisture mapping and AMSR-E validation using the PSR in SMEX02, *Remote Sens. Environ.*, *103*(2), 127–139.
- Burke, W. J., T. Schmugge, and J. F. Paris (1979), Comparison of 2.8- and 21-cm microwave radiometer observations over soils with emission model calculations, *J. Geophys. Res.*, *84*(C1), 287–294.
- Brunfeldt, D. R., and F. T. Ulaby (1986), Microwave emission from row crops, *IEEE Trans. Geosci. Remote Sens.*, *GE-24*(3), 353–359.
- Calvet, J. C., J. P. Wigneron, J. Walker, F. Karbou, A. Chanzy, and C. Albergel (2011), Sensitivity of passive microwave observations to soil moisture and vegetation water content: L-band to W-band, *IEEE Trans. Geosci. Remote Sens.*, *49*(4), 1190–1199.
- Chauhan, N. S. (2002), Soil moisture inversion at L-band using a dual-polarization technique: A model-based sensitivity analysis, *Int. J. Remote Sens.*, *23*(16), 3209–3227.
- Choudhury, B. J., T. J. Schmugge, A. Chang, and R. W. Newton (1979), Effect of surface roughness on the microwave emission from soils, *J. Geophys. Res.*, *84*(C9), 5699–5706.
- Crosson, W. L., A. S. Limaye, and C. A. Laymon (2005), Parameter sensitivity of soil moisture retrievals from airborne L-band radiometer measurements in SMEX02, *IEEE Trans. Geosci. Remote Sens.*, *43*(7), 1517–1528.
- Davenport, I. J., J. Fernández-Gálvez, and R. J. Gurney (2005), A sensitivity analysis of soil moisture retrieval from the tau-omega microwave emission model, *IEEE Trans. Geosci. Remote Sens.*, *43*(6), 1304–1316.
- De Jeu, R. A. M., and M. Owe (2003), Further validation of a new methodology for surface moisture and vegetation optical depth retrieval, *Int. J. Remote Sens.*, *24*(22), 4559–4578.
- Efron, B., and R. J. Tibshirani (1994), *An Introduction to the Bootstrap*, vol. 57, CRC Press, Boca Raton, Fla.
- Famiglietti, J. S., D. Ryu, A. A. Berg, M. Rodell, and T. J. Jackson (2008), Field observations of soil moisture variability across scales, *Water Resour. Res.*, *44*, W01423, doi:10.1029/2006WR005804.
- Gaur, N., and B. P. Mohanty (2013), Evolution of physical controls for soil moisture in humid and subhumid watersheds, *Water Resour. Res.*, *49*, 1244–1258 doi:10.1002/wrcr.20069.
- Heather M., et al. (2012), *Soil Moisture Active Passive Validation Experiment 2012 (SMAPVEX12) Experimental Plan*. Available at <https://smapvex12.espaceweb.usherbrooke.ca/home.php>.
- Jackson, T. J. (1993), III. Measuring surface soil moisture using passive microwave remote sensing, *Hydrol. Processes*, *7*(2), 139–152.
- Jackson, T. J., and P. E. O'Neill (1990), Attenuation of soil microwave emission by corn and soybean at 1.4 and 5 GHz, *IEEE Trans. Geosci. Remote Sens.*, *28*(5), 978–980.
- Jackson, T. J., and T. J. Schmugge (1991), Vegetation effects on the microwave emission of soils, *Remote Sens. Environ.*, *36*(3), 203–212.

- Jackson, T. J., and D. E. Le Vine (1996), Mapping surface soil moisture using an aircraft-based passive microwave instrument: Algorithm and example, *J. Hydrol.*, *184*(1), 85–99.
- Jacobs, J. M., B. P. Mohanty, E. C. Hsu, and D. Miller (2004), SMEX02: Field scale variability, time stability and similarity of soil moisture, *Remote Sens. Environ.*, *92*(4), 436–446.
- Jana, R. B., and B. P. Mohanty (2012), On topographic controls of soil hydraulic parameter scaling at hillslope scales, *Water Resour. Res.*, *48*, W02518, doi:10.1029/2011WR011204.
- Jones, M. O., L. A. Jones, J. S. Kimball, and K. C. McDonald (2011), Satellite passive microwave remote sensing for monitoring global land surface phenology, *Remote Sens. Environ.*, *115*(4), 1102–1114.
- Joshi, C., and B. P. Mohanty (2010), Physical controls of near-surface soil moisture across varying spatial scales in an agricultural landscape during SMEX02, *Water Resour. Res.*, *46*, W12503, doi:10.1029/2010WR009152.
- Kerr, Y. H., and E. G. Njoku (1990), A semiempirical model for interpreting microwave emission from semiarid land surfaces as seen from space, *IEEE Trans. Geosci. Remote Sens.*, *28*(3), 384–393.
- Lawrence, H., J. P. Wigneron, F. Demontoux, A. Mialon, and Y. H. Kerr (2013), Evaluating the semiempirical H-Q model used to calculate the L-band emissivity of a rough bare soil, *IEEE Trans. Geosci. Remote Sens.*, *51*(7), 4075–4084.
- McCabe, M. F., H. Gao, and E. F. Wood (2005), Evaluation of AMSR-E-derived soil moisture retrievals using ground-based and PSR airborne data during SMEX02, *J. Hydrometeorol.*, *6*(6), 864–877.
- Mo, T., B. J. Choudhury, T. J. Schmugge, J. R. Wang, and T. J. Jackson (1982), A model for microwave emission from vegetation-covered fields, *J. Geophys. Res.*, *87*(C13), 11229–11237, doi:10.1029/JC087iC13p11229.
- Narayan, U., V. Lakshmi, and E. G. Njoku (2004), Retrieval of soil moisture from passive and active L/S band sensor (PALS) observations during the Soil Moisture Experiment in 2002 (SMEX02), *Remote Sens. Environ.*, *92*(4), 483–496.
- Newton, R. W., Q. R. Black, S. Makanvand, A. J. Blanchard, and B. R. Jean (1982), Soil moisture information and thermal microwave emission, *IEEE Trans. Geosci. Remote Sens.*, *GE-20*(3), 275–281.
- Njoku, E. G., and J. A. Kong (1977), Theory for passive microwave remote sensing of near-surface soil moisture, *J. Geophys. Res.*, *82*(20), 3108–3118.
- Njoku, E. G., and S. K. Chan (2006), Vegetation and surface roughness effects on AMSR-E land observations, *Remote Sens. Environ.*, *100*(2), 190–199.
- Owe, M., R. de Jeu, and J. Walker (2001), A methodology for surface soil moisture and vegetation optical depth retrieval using the microwave polarization difference index, *IEEE Trans. Geosci. Remote Sens.*, *39*(8), 1643–1654.
- Pampaloni, P., and S. Paloscia (1986), Microwave emission and plant water content: A comparison between field measurements and theory, *IEEE Trans. Geosci. Remote Sens.*, *GE-24*(6), 900–905.
- Panciera, R., J. P. Walker, and O. Merlin (2009), Improved understanding of soil surface roughness parameterization for L-band passive microwave soil moisture retrieval, *IEEE Trans. Geosci. Remote Sens. Lett.*, *6*(4), 625–629.
- Peel, M. C., B. L. Finlayson, and T. A. McMahon (2007), Updated world map of the Köppen-Geiger climate classification, *Hydrol. Earth Syst. Sci.*, *4*(2), 439–473.
- Saleh, K., J. P. Wigneron, P. Waldteufel, P. De Rosnay, M. Schwank, J. C. Calvet, and Y. H. Kerr (2007), Estimates of surface soil moisture under grass covers using L-band radiometry, *Remote Sens. Environ.*, *109*(1), 42–53.
- Saltelli, A., S. Tarantola, F. Campolongo, and M. Ratto (2004), *Sensitivity Analysis in Practice: A guide to Assessing Scientific Models*, John Wiley, Chichester, U. K.
- Saltelli, A., M. Ratto, T. Andres, F. Campolongo, J. Cariboni, D. Gatelli, and S. Tarantola (2008), *Global Sensitivity Analysis: The Primer*, John Wiley, Chichester, U. K.
- Santi, E., S. Pettinato, S. Paloscia, P. Pampaloni, G. Macelloni, and M. Brogioni (2012), An algorithm for generating soil moisture and snow depth maps from microwave spaceborne radiometers: HydroAlgo, *Hydrol. Earth Syst. Sci.*, *9*(3), 3851–3900.
- Schmugge, T. J. (1983), Remote sensing of soil moisture: Recent advances, *IEEE Trans. Geosci. Remote Sens.*, *GE-21*(3), 336–344.
- Schmugge, T. J., and B. J. Choudhury (1981), A comparison of radiative transfer Models for predicting the microwave emission from soils, *Radio Science*, *16*, 927–938.
- Schmugge, T., P. Gloersen, T. Wilheit, and F. Geiger (1974), Remote sensing of soil moisture with microwave radiometers, *J. Geophys. Res.*, *79*(2), 317–323.
- Schmugge, T., P. E. O'Neill, and J. R. Wang (1986), Passive microwave soil moisture research, *IEEE Trans. Geosci. Remote Sens.*, *GE-24*(1), 12–22.
- Seo, D., T. Lakhankar, and R. Khanbilvardi (2010), Sensitivity analysis of b-factor in microwave emission model for soil moisture retrieval: A case study for SMAP mission, *Remote Sens.*, *2*(5), 1273–1286.
- Ulaby, F. T., M. Razani, and M. C. Dobson (1983), Effects of vegetation cover on the microwave radiometric sensitivity to soil moisture, *IEEE Trans. Geosci. Remote Sens.*, *GE-21*(1), 51–61.
- Ulaby, F. T., R. K. Moore, and A. K. Fung (1986), *Microwave Remote Sensing Active and Passive-Volume III: From Theory to Applications*, Addison-Wesley, Reading, Mass.
- Van de Griend, A. A., and M. Owe (1994), Microwave vegetation optical depth and signal scattering albedo from large scale soil moisture and Nimbus/SMMR Satellite observations, *Meteorol. Atmos. Phys.*, *54*, 225–239.
- Van de Griend, A. A., and J. P. Wigneron (2004), The b-factor as a function of frequency and canopy type at H-polarization, *IEEE Trans. Geosci. Remote Sens.*, *42*(4), 786–794.
- Wang, J. R., P. E. O'Neill, T. J. Jackson, and E. T. Engman (1983), Multifrequency measurements of the effects of soil moisture, soil texture, and surface roughness, *IEEE Trans. Geosci. Remote Sens.*, *GE-21*(1), 44–51.
- Wigneron, J. P., L. Laguerre, and Y. H. Kerr (2001), A simple parameterization of the L-band microwave emission from rough agricultural soils, *IEEE Trans. Geosci. Remote Sens.*, *39*(8), 1697–1707.
- Wigneron, J. P., A. Chanzy, Y. H. Kerr, H. Lawrence, J. Shi, M. J. Escorihuela, and K. Saleh-Contell (2011), Evaluating an improved parameterization of the soil emission in L-MEB, *IEEE Trans. Geosci. Remote Sens.*, *49*(4), 1177–1189.
- Wilheit, T. T. (1978), Radiative transfer in a plane stratified dielectric, *IEEE Trans. Geosci. Remote Sens.*, *16*(2), 138–143.
- Zhixiong, L., C. Nan, U. D. Perdok, and W. B. Hoogmoed (2005), Characterization of soil profile roughness, *Biosyst. Eng.*, *91*(3), 369–377.